Eindhoven University of Technology

Eindhoven University of Technology

MASTER

Thermoacoustic stability of combustion in central heating boilers

Looijmans, J.M.M.

Award date:
2010

Link to publication

**Thermoacoustic stability of combustion
in central heating boilers**

WVT 2010.11

J.M.M. Looijmans
531400

Master's Thesis

Supervisor:
Professor P.H. de Goey

Coaches:
dr. V.N. Kornilov
M. Manohar, MSc.

Eindhoven University of Technology
Department of Mechanical Engineering
Combustion Technology Group

October 21, 2010

Abstract

In the last decades public awareness let to a negative opinion about burning fossil fuels, because of the effects on the environment. To reduce emissions the combustion temperature needs to be decreased. This can be effectively done by burning a fuel lean mixture. This strategy comes at a cost, as burner devices, are vulnerable to acoustic instabilities while burning a lean mixture. This problem increases the costs and time needed to design and refine new heating equipment.

Combustion driven oscillations are caused by a feedback loop that is formed between the heat release and the system acoustic modes. The flames act as a power supply for the noise which have an influence on the gasses which will burned. Because the goal of this study is to gain more knowledge about these oscillations (noise), the thermoacoustic behavior of the system as well the thermoacoustic effects of combustion are studied.

First the effect of the flame is studied. The flame can be varied with different parameters like equivalence ratio and velocity, which results in different flame transfer function. Subsequently the burner pattern is studied. Furthermore devices, introduced to enhance the uniformity of the flame on the burner deck, are studied. These devices include a swirler plate and a distribution plate and have an effect on the flame transfer function.

For studying the boiler a setup was created to introduce excitation and measure the frequency response. For several parts of the boiler the effect on the frequency response is measured, like the exhaust, the inlet and several connecting elements. After the boiler was installed, the effect of ignition is studied, as well as the temperature of the water in the heat exchanger. Measurements are done for different heat intensities.

As information about the flame and the burner system are used for (in)stability prediction, for a more accurate prediction a model is needed. Software developed at the Eindhoven University of Technology is used and modified in order to calculate the acoustic response of the model. A start is made on the boiler model.

Contents

List of Figures

Chapter 1

Introduction

In the present world power generation is mainly done by the combustion of fossil fuels. Due to public awareness about the environment a negative opinion is formed in the last decades about burning fossil fuels. In order to decrease the pollution, strong policies have come into effect to decrease the pollutant emissions of industrial as well as household equipment. Part of the pollution are the NO_x emissions. To reduce these emissions the combustion temperature needs to be decreased. This can be effectively done by burning a fuel lean mixture, and this has been widely adopted by the industry. However, this strategy comes at a cost, as burner devices, especially household burners, are vulnerable to acoustic instabilities while burning a lean mixture. This problem increases the costs and time needed to design and refine new heating equipment. Predicting these thermoacoustic oscillations has therefore become very important for the manufacturers of the boiler systems and burner manufacturers like Polidoro.

The acoustic oscillations occur in almost every combustion process. The statement made by Putnam in the preface of his book [1] is still actual:

> "Combustion systems often generate acoustical oscillations; these oscillations not only may be annoying, but at times may become so violent as to damage or destroy the equipment. It is difficult, if not impossible, to design a combustion chamber in such a way that no oscillation can occur."

Combustion driven oscillations are caused by a feedback loop that is formed between the heat release and the system acoustic modes. The flames act as a power supply for the noise which have an influence on the gasses which will burned. Because the goal of this study is to gain more knowledge about these oscillations (noise), the thermoacoustic behavior of the system as well the thermoacoustic effects of combustion are studied.

As stated above the acoustic (in)stability is the result of interaction between the burner and the boiler (the burner system). To determine which burner is acoustically stable, Polidoro installs a boiler and tries a large number of different burners. The aim of this study is to get more knowledge about this instability in order to diminish the number of burners that has to be tested. In this chapter an overview of the theory behind this study is given.

1

1.1   Thermoacoustic instabilities

The oscillations, or noise, can be classified by character: i) combustion roar and ii) combustion driven oscillations. Combustion roar does not have a specific frequency, but rather a broad spectrum of noise and is generated during turbulent combustion. Because the flames in this study are laminar and thus does not generates roar, this type of flame noise will not be discussed.

Combustion driven oscillations are generally more obvious when they occur and usually have a specific frequency which corresponds to the burner system. It is still common practise to remove these oscillations (noise) from the burner system by trail-and-error. Because this is very time consuming, this study aims to develop a method to predict instabilities in order to shorten the time to design and refine the heating equipment.

Several studies have been conducted in recent years on the subject. An overview of the subject is done by Candel, who summarized various studies on the interaction between acoustics and flames [2]. Lieuwen wrote a review on methods of modeling of acoustically perturbed flow and flame [3]. At the Eindhoven University of Technology the effect of different conditions for different burner patterns [4, 5] is studied. This study is focussed on the influence of the pattern of the burner plate and the influence of a distribution plate before the burner plate. This will be discussed further in Chapter 2.

1.1.1   Rayleigh criterion

In order to study the combustion driven oscillations in a burner system, a description is needed which connects the flame with the acoustics. The first to explain the mechanism of energy transfer from the flame to acoustical mode was Lord Rayleigh in 1878. Rayleigh gave a more detailed description of his criteria in [6]:

> "If heat be periodically communicated to, and abstracted from, a mass of air vibrating (for example) in a cylinder bounded by a piston, the effect produced will depend upon the phase of the vibration at which the transfer of heat takes place. If heat be given to the air at the moment of greatest condensation or to be taken from it at the moment of greatest rarefaction, the vibration is encouraged. On the other hand, if heat be given at the moment of greatest rarefaction, or abstracted at the moment of greatest condensation, the vibration is discouraged."

The first to describe this criterion in mathematical form was Putnam [7]:

$$R = \frac{1}{T} \int\limits_T q'(t)\, p'(t)\, dt. \tag{1.1}$$

This describes the power transferred from the oscillating heat release rate q' to the pressure oscillations p'. T is the period of the oscillation. This expression assumes that the oscillating

heat release is distributed over a volume in which the oscillating pressure is uniformly distributed. If not, an integral over that volume is required.

According to equation 1.1, when the Rayleigh index (R) is positive, thermoacoustic oscillations will grow and when R is negative, the oscillations will be damped. However, Equation 1.1 does not take into account damping in the system. If damping exists, the Rayleigh index should be large enough to overcome the losses for the oscillations to grow.

1.1.2 Transfer function of flames

In Section 1.1.1 an explanation was given on the prediction of instabilities in combustion systems. This method needs information about how the flame responds on acoustical perturbations upstream of the flame. In this section a popular method how to describe this flame response is presented.

The idea to use a transfer function to characterize the response of the flame to the acoustic perturbation is popular in the science of system control. In a system control problem the system is a black box, like in this problem the flame is. Via a transfer function, the relation between the input and output is described. In this problem the acoustic perturbation is the input and the flame response is the output. In this study premixed flames are used. For premixed flames it is assumed that the flame response scales linearly with the upstream acoustic perturbation. Other variables have a small or no influence on the flame response [8]. The complex flame transfer function is defined as:

$$TF(f) = \frac{q'(f)/\bar{q}}{u'(f)/\bar{u}} \tag{1.2}$$

where $q'(f)$ is the flame response, $u'(f)$ is the upstream acoustic perturbation, $\bar{q}$ is the mean heat release rate and $\bar{u}$ the mean velocity. The ratio $\bar{q}/\bar{u}$ is introduced to normalize the transfer function. That means that the transfer function is the relative flame response divided by the relative acoustic perturbation.

An example of how a flame transfer function is represented, is described in Chapter 2.

1.1.3 Implementation of the flame transfer function

The calculated or measured transfer function is used in system control theory for system control and system instability prediction. A popular way of formulating the transfer function is the so-called $(n - \tau)$ representation [9]. In this representation, n describes the sensitivity of the combustion heat release to pressure oscillation and τ stands for the time lag between the acoustic perturbation and the corresponding heat release oscillation. In other words, n is related to the gain of the transfer function (Equation 1.2) and τ is related to the phase delay. In this subsection the transfer function is implemented in the Rayleigh integral.

In the Section 1.1.1 the Rayleigh index was defined as a function of p'. And in section 1.1.2 the transfer function is defined as a function of u'. The pressure oscillation p' and the air speed oscillation u' are linked via the calculation of impedance. The acoustic impedance is defined as :

$$z = \frac{p'}{u'}. \tag{1.3}$$

Furthermore expression 1.2 can be rewritten so that the variable heat release is given as a function of the flame response as $q' = TFu'\bar{q}/\bar{u}$. Substituting this expression and Expression 1.3 into Expression 1.1 gives:

$$R = TF\frac{\bar{q}}{\bar{u}}z\left(\frac{1}{T}\int_T (u')^2 dt\right). \tag{1.4}$$

The upstream velocity oscillation is assumed to be periodic ($u' = \hat{u}\sin(\omega t)$). This can be inserted into Equation 1.4. Integrating this new equation gives a new expression for the Rayleigh index:

$$R = \frac{\bar{q}}{2\bar{u}}z(f)\,TF(f)\,\hat{u}^2. \tag{1.5}$$

It should be noted that values for $\hat{u}, \bar{q}$ and $\bar{u}$ are absolute values. Therefore, the phase difference between the transfer function and the acoustic impedance ($z(f)$) will determine the sign of the Rayleigh index and the growth rate of the thermoacoustic instabilities will be the result of the difference in gain between the two signals. If the Rayleigh index is larger than the damping of the system it will lead to instabilities.

1.2   System instabilities

The Section 1.1.1 focussed on the influence of flames on the thermoacoustic instabilities and a method was presented to describe these instabilities. However, the flame is only one half of the problem, as the instabilities are caused by the interaction between the heat source and burner system. This section explains how the acoustic properties of the boiler system are determined. With the information of the burner system, but also the information of the flame a prediction can be made about stability of the boiler. The information of both can also be used to construct a model for even better prediction.

In order to determine the acoustic properties of the boiler, the air in the system is excited by an external acoustic source. The response in the boiler to this excitation is measured near the excitation input as a reference and at a point inside the boiler, near the burner. With this the frequency response of the boiler can be measured. The relation between the input oscillations and the response can be described as follows:

$$TF(f) = \frac{p_2}{p_1} \tag{1.6}$$

where p_1 is the pressure signal of the reference signal as is p_2 the other pressure signal. This can be used to measure the effect of different boiler parts on the acoustic signature. More on this subject can be found in Chapter 3.

1.3 System model

As stated in Section 1.2, for a better estimation of system instabilities a model is necessary. It is convenient to use the oscillations in the system as variables. The oscillations can be described using the wave equation for pressure disturbances [10]:

$$\frac{\partial^2 p'}{\partial t^2} = c^2 \frac{\partial^2 p'}{\partial x^2} \tag{1.7}$$

Here, p' is the pressure oscillation, t is time, x is the distance and c is the speed of sound. When integrated, this results in:

$$\frac{p'(x,t)}{\rho c} = f(x - ct) + g(x + ct) \tag{1.8}$$

with f and g being the Riemann invariants which represent the oscillations moving with the speed of sound in the positive and negative direction. If the wave equation for velocity disturbances is solved, one finds:

$$u' = f - g \tag{1.9}$$

Now the Riemann invariants f, g can be expressed in terms of p', u';

$$f = \frac{1}{2} \left(\frac{p'}{\rho c} + u' \right) \tag{1.10}$$

$$g = \frac{1}{2} \left(\frac{p'}{\rho c} - u' \right). \tag{1.11}$$

In these equations, ρ is the mean gas density and c is the speed of sound. For ducts with constant cross-section, it is convenient to use the Riemann invariants to describe the solution structure in terms of harmonic disturbances that propagate with and against the mean flow, respectively. With these equations a solution can be found for a network of acoustic elements. This is explained in Chapter 4.

1.4   Thesis outline

The aim of this study is to get more knowledge about the origin of acoustic instabilities in a combustion system, with the goal to predict these instabilities. As the problem consists of both the flame and the burner system (the boiler), information is needed about the acoustical properties of the flame and of the boiler. Additionally, with this information a model of the system can be constructed for more accurate prediction. Chapter 2 gives more insight into flame transfer function measurements. Although different studies have been done on this subject, this study will introduce new parameters to investigate. Burners used in current heating equipment are studied. Chapter 3 provides more insight into frequency response measurements on the boiler. This chapter goes into acoustic response of different parts of the boiler on the frequency response. Chapter 4 describes how the modeling software works and a start is made on modeling the boiler.

Chapter 2

Flame transfer function

As mentioned in Chapter 1, household burner devices are very sensitive to acoustic oscillations. In order to prevent these oscillations from occurring, manufacturers of burners are trying different strategies. With more knowledge about the flame, a flame can be chosen which will prevent the oscillations from occurring. Different studies have been done on the effects of several parameters on the flame transfer function. Because the manufacturers of burners are trying different burners to prevent the acoustical oscillations from happening, the influence of different burner patterns is investigated.

In order to predict acoustical instabilities, more information about both the system and the flame is needed. This chapter presents the experimental setup and the results of experiments.

2.1 Experimental setup

In order to measure the transfer function of a flame several parameters need to be controlled and others need to be measured. For the incoming gas it is important to control the equivalence ratio and the thermal power of the flame. The thermal power is modulated via the gas velocity. Also the upstream perturbation need to be provided in a controlled manner, both the frequency and the amplitude. Measurements are needed on the oscillating velocity and the oscillating heat release, in order to determine the transfer function.

2.1.1 Equipment

With these requirements in mind an experimental setup is realized. The basis of this setup is a straight tube. On top of the tube is the burner deck, on the bottom of the tube a loudspeaker is installed. On the burner deck different burners can be placed. The loudspeaker is connected to a amplifier in order to provide a pure tone as the upstream perturbation. The gas flow rate and the equivalence ratio of the gas are controlled by Mass Flow Controllers (MFC). These MFCs are positioned far upstream of the burner to provide perfect mixing. Experiment parameters use the velocity u for speed, but in case of varying porosity mass flow

rate is used. Methane is used for all experiments.

In order to measure the oscillation of the gas flow a hot wire anemometer was installed 25 mm upstream of the burner deck. The anemometer is as small as possible in order to minimize its influence on the gas flow. Also a distance between the burner deck and the anemometer is created to further decrease the effect of the anemometer on the flow. The oscillating heat release is measured via an indicator, because it can not be measured directly. Because the chemiluminescence intensity of OH of a flame subjected to acoustic perturbation is correlates with the oscillating heat release, it is chosen as an indicator and is measured via a photo-multiplier tube (PMT). The PMT is equipped with a filter so only light that has the same wavelength as OH is detected. The PMT is positioned at 30 cm from the flame and aimed directly at it, so that the whole flame can be seen by the PMT.

All the equipment (PMT, hot wire anemometer, MFCs and the loudspeaker) are connected to a computer via a data acquisition card (National Instruments BNC 2111) to control the incoming gas flow and upstream perturbation, but also to measure the perturbation and oscillating heat release. Software specially designed for this setup is used for the control and measurement of the signals. A schematic overview of the setup can be seen in Figure 2.1.
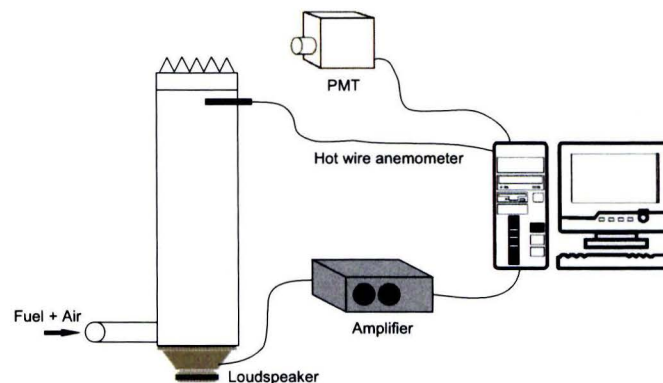
Figure 2.1: Layout of the setup for flame measurements

2.1.2   Calculating flame transfer function

For transfer function determination a pure tone excitation ranging from 30 to 600 Hz with a step size of 10 Hz is used. Measurements are done of the hot wire anemometer and the PMT with a sampling frequency of 25 kHz, for 0.66 seconds. After the measurements are done the data needs to be processed in order to calculate the flame transfer function gain and phase. It is necessary to calculate the gain of the transfer function from the fourier transformation of the raw data because of the influence of noise and the nonlinear response of the flame heat release. Furthermore, the law of energy conservation requires that the gain is equal to one for the quasi-stationary response of the oscillating heat release to the gas flow oscillation. The normalization factor found at quasi-stationary condition can be used to scale the transfer

function at other frequencies.

The phase can be calculated by applying a cross-correlation analysis between the signals of the heat release oscillation and the gas velocity variation. The cross-correlation function (CCF) can be expressed by Equation 2.1:

$$CCF(\tau) = \frac{1}{T} \int_{T_1}^{T_2} Q'(t)V'(t+\tau)dt \qquad (2.1)$$

With this equation the phase lag between $Q'(t)$ and $V'(t)$ can be calculated, as the time between T_1 and T_2 where $CCF(\tau)$ has the first maximum is that phase lag.

2.1.3 Representation of flame transfer function

The flame transfer function can be visualized in different ways. The method used most frequently in this report is shown in Figure 2.2. In the top graph the gain is plotted against the frequency, in the bottom graph the phase against the frequency is depicted.
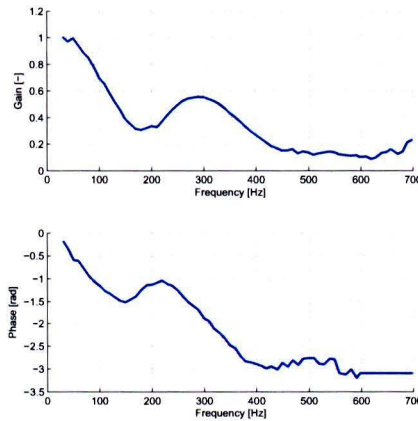
Figure 2.2: Example of visualization of flame transfer function

In Chapter 1 it is explained that the gain influences the growth rate of the thermoacoustic instabilities and the phase affects the sign of the growth rate. It should be noted that no measurements are done at a frequency lower than 30 Hz. This is because the loudspeaker used is not able to produce these low frequencies. It is clear that the gain goes to 1 when the frequency goes to 0, because when there is no perturbation, the input and the output are the same. To get this effect, the normalization mentioned in Section 1.1.2 is necessary. Furthermore no measurements are done with a higher frequency than 700 Hz, because the signal to noise ratio will become too low.

2.2   Results and discussion

In Section 2.1 the measurement setup and processing is explained. This section presents the results of the experiments and discusses the results. The results can be divided in three separate parts. The first part discusses the results of different lay-outs of the burner plate, the second part discusses the experiments done on a burner with different distribution plates and the third part the difference between a simple burner with distribution devices.

2.2.1   Effects of flame parameters

Although there have been different studies into the effects of different burning conditions, it acts as an example for the rest of the results. It gives a good example on how the flame transfer function responds to parameters like equivalence ratio. Equivalence ratio is the actual fuel-to-oxidizer ratio to the stoichiometric fuel-to-oxidizer ratio. The flame used is a laminar premixed Bunsen type flame. A burner plate is used which holds the middle between a single bunsen flame and a burner plate with a pattern used in current heating equipment. The burner plate used is shown in Figure 2.5.a.
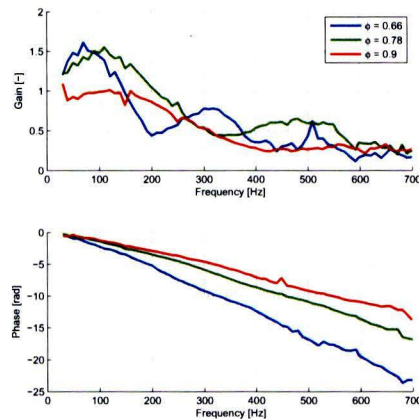
Figure 2.3: Gain and phase of flame transfer function for simple burner plate with varying equivalence ratio and $\dot{m} = 1.6$ l/min

First the effects of varying equivalence ratios ϕ are analyzed. The results are shown in Figure 2.3. The gain of the transfer function develops similarly for each of the three cases, but the first dip for the curve of $\phi = 0.66$ is located at 200 Hz, for $\phi = 0.78$ at 220 Hz and for $\phi = 0.99$ at 450 Hz. There is also an effect on the phase delay. For higher frequencies the phase delay is smaller. This is an expected effect as the phase delay scales with the flame height over the air velocity, or $\tau \sim h/u$. Lower equivalence ratios give a higher flame and thus a larger phase delay. Both these effects can be useful when selecting a burner for a boiler system. The equivalence ratio can be chosen such that the growth rate is smaller then the damping in

the system or that the sign of the Rayleigh index is negative so that no instabilities will occur.
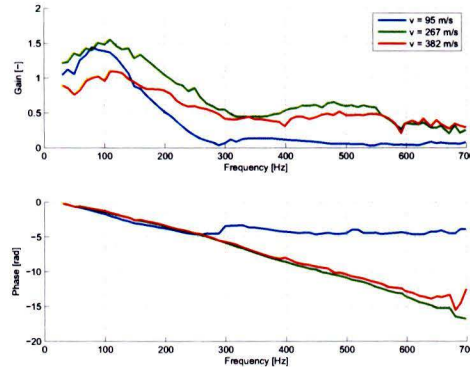
Figure 2.4: Gain and phase of flame transfer function for simple burner plate with varying air velocity and $\phi = 0.78$

Another parameter that has a direct influence on the flame is the velocity of the incoming air. This is also studied and the results are shown in Figure 2.4. It is shown that small variations in velocity has a small effect on the gain of the flame transfer function. The spike is at the same frequency. Biggest difference is that for the lowest speed the gain drops to almost zero for higher frequencies. If the variations in speed are small enough, the phase delay does not change, as $\tau \sim h/u$. If the variation is large enough a tipping point is reached where phase delay remains constant from a certain frequency onward. This effect is explained by Kornilov [8].

Now that the influence of different flame parameters is described, different burner patterns are analyzed and compared in the next section.

2.2.2 Effects of different burner plate lay-outs

In Section 2.2.1 the influence of the mass flow rate and equivalence ratio is analyzed. In this section the influence of different burner plate lay-outs is reviewed. To create different burner patterns, there can be an endless variation in hole diameter, distance between the holes (pitch) and porosity of the burner plate. A first point of interest is the difference in flame transfer function of the simple burner, and two types of burner pattern used by industry. The studied patterns are shown in Figure 2.5. The three burners shown have a similar porosity. The burner pattern with slits and holes (Figure 2.5b) and fiber(Figure 2.5c) are used in commercial available heating systems.

In recent history several studies have been done on the flame transfer function of multiple flames anchored on a perforated burner deck with holes of 2 and 3 mm [11, 12]. Because the influence of variations to the simple burner plate (Figure 2.5.a) has been described by Kornilov [5], this study goes into multiple flames anchored on a burner deck, however perforations will be small holes (smaller than 2 mm) and multiple slits. An example is shown in Figure 2.5b. Also the burner pattern shown in Figure 2.5c is studied, especially the influence

(a) Simple burner   (b) Burner with slits and holes   (c) Burner with fiber
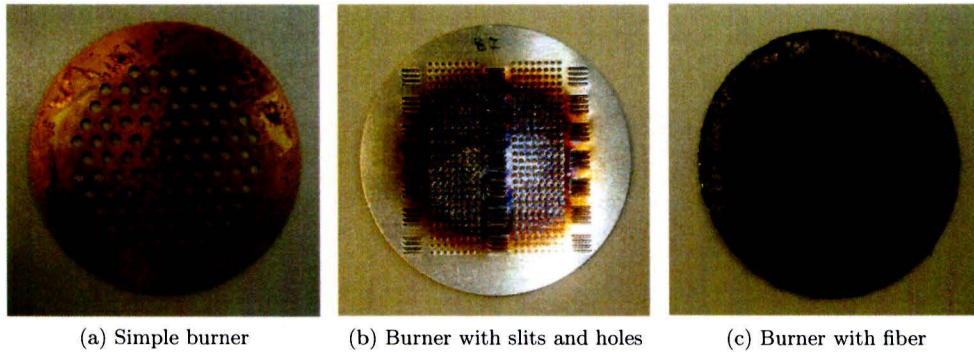
Figure 2.5: Burner plates used explaining their influence on flame transfer function

of the orientation of the fabric on the flame transfer function.

For burner patterns similar to the pattern in Figure 2.5b it is interesting to see if these patterns have the same response to a variation in flame parameters like equivalence ratio.
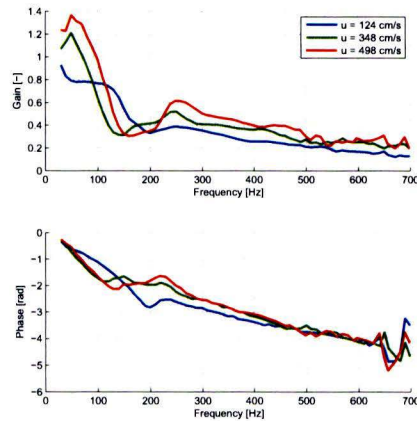
Figure 2.6: Gain and phase of flame transfer function for industrial burner plate with varying mass flow rate and $\phi = 0.78$

The results are shown in Figure 2.6, where it can be seen that the response to a change in velocity is similar as that of the simple burner plate for the higher velocities. Difference is that the spike at the lowest frequency not occur. The phase delay for the different velocities is the same, which is expected as $\tau \sim h/u$. Difference in the phase delay is the small dip at different frequencies which corresponds to the dip in the gain. The variation in incoming air velocity was not high enough to see the leveling in phase delay, as is seen with the simple burner plate. The plot with constant velocity and varying equivalence ratio compares with this result, no spike in the gain plot for low equivalence ratio and smaller phase delay for

higher velocity.

Figure 2.7: Gain and phase of flame transfer function for three different industrial type burner plates, $\phi = 0.78$, $\dot{m} = 1.6$ l/min

The layout of this burner can be varied in many ways. For these experiments burner patterns are used which are similar to the burner in Figure 2.5b, but vary by different porosity (less holes) and different position of the slits. In Figure 2.7 burner patterns are compared. As the patterns are similar, it is expected that the acoustic signature of the flame are also similar. This holds for burner pattern 208 and 246 (green and red curve respectively), but the gain of the transfer function of pattern 87 is much lower. Also the phase delay of this pattern is much larger than that of the other patterns. Visual inspection of the flame of the different cases did not reveal any differences. Although it not known what causes this difference, it is clear that different burners have a different flame transfer function.

The fiber material used on the industrial type burner (Figure 2.5c) is knitted into a fabric, which can be used in various ways. For the experiments the fabric was fastened to a burner plate (with the same pattern as the burner from Figure 2.5b) with the knitting pattern parallel to the burner pattern, perpendicular to the burner pattern and upside down and perpendicular to the burner pattern. It is expected that the response of the three different burners is similar (the flame height should be the same as the porosity is the same).

Figure 2.8 shows the representation of the flame transfer function for the three different burners. The transfer function is almost identical for higher equivalence ratios and lower speeds. The phase delay for the burner with the knitted fiber pattern perpendicular to the burner plate pattern is lower, probably caused by lower flame length. It is assumed that the air travels more easily through this burner which results in a lower air velocity, which results in a shorter flame. However, this can not be visually confirmed because the knitted fibers cause a flame bed with no visual flame. At higher frequencies the values of the flame transfer function are small and this in combination of data processing results in the choppy displays of the phase delay.
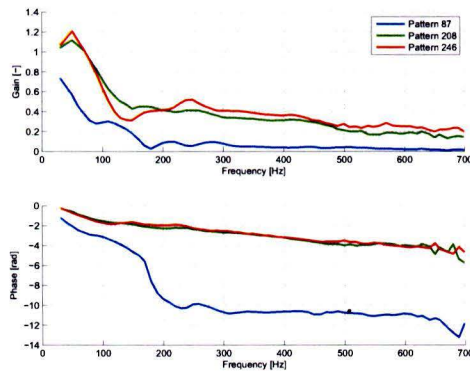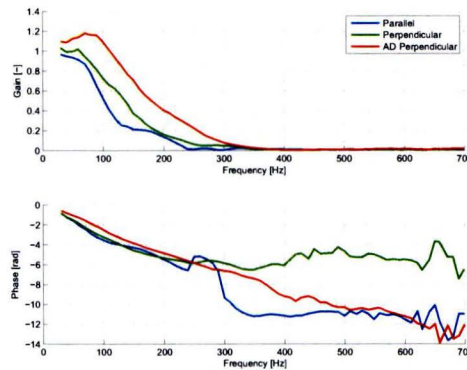
Figure 2.8: Gain and phase of flame transfer function for three different industrial type burner plates with fiber, $\phi = 0.66$, $\dot{m} = 2.29$ l/min

To conclude the measurements on different burner patterns it is interesting to show the differences in flame transfer function for the three different burners, as shown in Figure 2.5. This underlines the statement that different burners have a different effect on the flame transfer function, and thus a different effect on stability of the heating system.
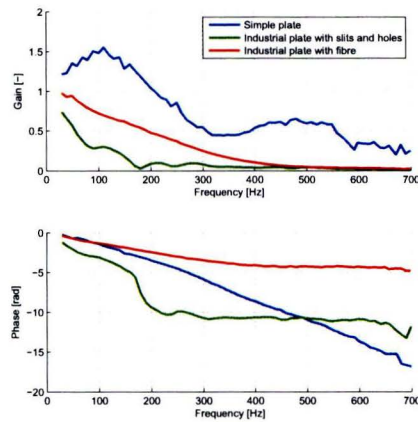
Figure 2.9: Gain and phase of flame transfer function of different burner plates, $\phi = 0.78$, $\dot{m} = 1.6$ l/min

From Figure 2.9 can be derived that there is a big difference between the different burner patterns. The results show for the burner pattern with fiber (Figure 2.5c) a smaller phase delay. This is expected, as it is not a flame, but more like a flame bed with a lower maximum air velocity exiting the burner plate, resulting in a lower flame length. Another characteristic about the phase plot of the industrial burner with slits and holes is the the steady phase delay drop for low frequencies, a big drop around 200 Hz and then constant for higher frequencies.

In this section the influence of different burner patterns has been investigated. In the next section the influence of upstream air distributors is looked into.

2.2.3 Effects of distributor

The burner used in current heating equipment is a three-dimensional shape, a cylinder, closed at one end, and the air-fuel mixture coming in at the other end with flames attached to the side of the cylinder, on the burner pattern. The burner pattern is similar to that of the burner shown in Figure 2.5b). An example of such a burner is shown in Figure 2.10a.

(a) Industrial burner   (b) Distributor   (c) Swirler
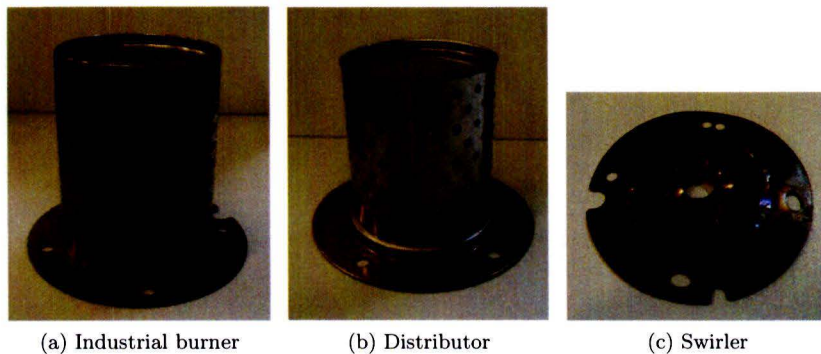
Figure 2.10: The burner used in heating equipment, the distributor and the swirler

It is necessary to distribute the incoming air-fuel mixture evenly over the surface of the burner. If the gaseous mixture is not evenly distributed this can result in an inhomogeneous flame. This means that the flame length can be of different size on the burner surface. In its turn this can lead to different flame transfer functions.

To create a uniform flame on the burner surface two devices have been introduced. In Figure 2.10b a distributor is shown. As the air-fuel mixture enters the burner at the bottom, the distributor creates an extra pressure drop and thus prevents more gas flowing out at the bottom of the burner and more gas at the top. So in theory the distributor creates a more uniform flame on the burner deck. It is expected that the distributor also has an influence on the flame transfer function. With the distributor plate as new variable, this chapter studies the effect of the distribution plate on the flame transfer function. The effect of the swirler, shown in Figure 2.10c, is also studied. This is explained in Section 2.2.4.

To test the influence of the distribution plate a sample was created as depicted in Figure 2.5b, but with a distribution plate like the real burner. For this experiment the real burner is used, instead of the flat samples in previous experiments. Earlier experiments have shown that measuring the flame transfer function of a three dimensional burner gives the same result as measurements done on a flat burner plate. These patterns used for this comparison (pattern number 83 and 101) are very similar. The two patterns are shown in Section A.1. The distribution plate used here is identical.
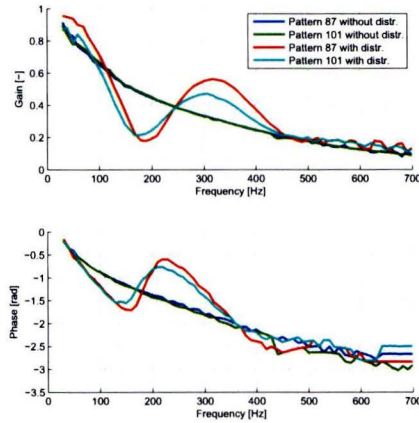
Figure 2.11: Comparison of pattern with and without distribution plate, u = 75 m/s, $\phi = 0.9$

In Figure 2.11 the results are shown for the comparison between a flame transfer function of a burner with and burner without distribution plate. The difference between a single burner plate and a burner plate with distribution plate is substantial. This is caused by the difference in velocity of the gas. The porosity of the distribution plate is much smaller than that of a burner plate, causing longer and shorter flames on the burner deck; at the position of a hole in the distribution plate, the flame on the burner deck is longer. This is shown in Appendix A.2. If the velocity is set to a higher value, or the lower equivalence ratios, the flames are longer and the effect is less.
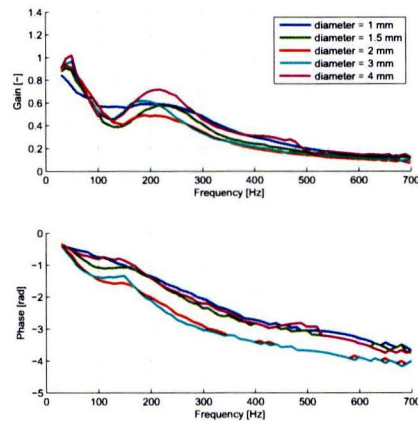
Figure 2.12: Different distribution plates with different hole sizes, porosity ≈ 0.136, u = 75 cm/s, $\phi = 0.9$

To get more information about the influence of the distribution plate layout on the flame

transfer function, the effect of two parameters of the distribution plate are studied. In the first experiment the effect of the layout is investigated. This means that the porosity of the distribution plate is kept constant, while the size of the holes are varied.

The results are shown in Figure 2.12. From this figure it can be concluded that the influence of the influence of the hole size is small. The flame transfer is similar, the gain and phase response only have small variations between the different distribution plates. This is as expected, because it was assumed that the flame length would be similar. The visual inspection of the flames met this assumption. However there is a small difference in phase delay, up to 1 rad in the range of 200 to 700 Hz. To explain this further research is needed.

Another way to alter the properties of a burner with distribution plate is to vary the porosity of the distribution plate. For the most clear comparison the hole diameter was kept constant, although previous experiment showed that the hole diameter does not have a large influence on the flame transfer function. However, including other distribution plates does not result in a different conclusion.
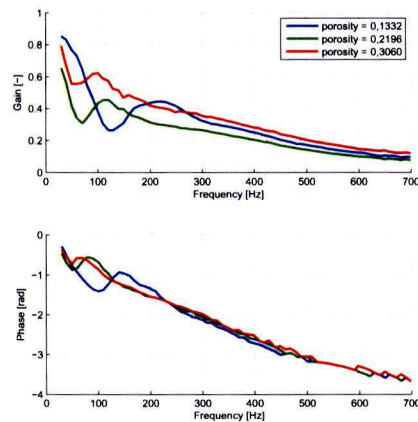
Figure 2.13: Different distribution plates with different porosity, hole diameter = 2 mm, u = 75 cm/s, $\phi = 1.0$

In Figure 2.13 the results are shown. For the burner patterns used, several distribution plates result for the flame transfer function in a dip and a peak in both the gain and phase delay, but the position in the frequency domain varies. For decreasing porosity this dip moves to a higher frequency. This can be used to cancel out an instability of a system at a specific frequency.

The final parameter that is studied in this thesis is the influence of the distance between burner plate and distribution plate on the flame transfer function. The initial distance used between the burner plate and the distribution plate was copied from the burners used in boiler systems by Polidoro. The reason for this distribution plate is explained earlier in this

section. But why this specific distance between burner plate and distribution plate (4 mm) was chosen is not known.
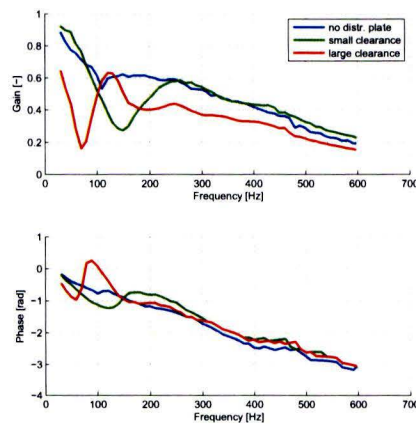
Figure 2.14: Different distances between burner plate and distribution plate, u = 75cm/s, ϕ = 1.0

The results are shown in Figure 2.14. The first point to notice is that the phase is positive of the flame transfer function at 90 Hz for the largest distance between burner plate and distribution plate. Physically it is not possible, as it would mean that the flame responds to the acoustic perturbation before the perturbation reaches the flame. Probably the phase lag will go to almost zero and the effect in the figure is the result of measurement inaccuracy.

Further, it can be observed that an increasing distance has the same effect as increasing the porosity. If the flame is visually studied, with the distribution plate at a small distance, the flame on the burner plate is bigger at the position where there is a hole in the distribution plate. A picture of this effect is included in Section A.2. But as the distance increases, the air-fuel mixture gets more time to distribute itself over the burner plate. This results in a more homogeneous flame on the burner plate; the difference in flame length is less. If the distance between the distribution plate and burner plate is increased further and further, at some point the effect of the distribution plate is gone. It will be like a burner plate without a distribution plate upstream.

2.2.4   Effects of swirler plate

Because it is necessary to distribute the incoming air-fuel mixture evenly over the burner area, two devices are used. In Section 2.2.3 the influence of the distribution plate on the flame transfer function is studied. In this section the effect of the swirler plate is studied. An example of the swirler plate used by Polidoro is shown in figure 2.10c.

The flame transfer function of the burner is measured with a burner like the one shown in Figure 2.10a, as it is not possible to create a flat burner with swirler plate. Experiments have shown that the measurements done on a flat sample and a real burner give the same result. But while the flat burner samples are easier to handle and measure, these are used when possible.
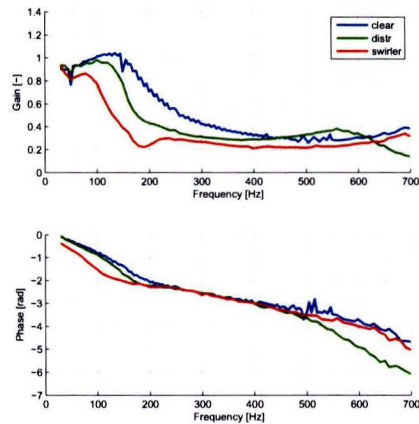
Figure 2.15: Effect of mixing devices on flame transfer function, u = 75 cm/s, ϕ = 0.75

The results of measurements of the flame transfer function of different mixing devices is shown in figure 2.15. The differences in flame transfer function between the different mixing devices is significant for low frequencies. That there is a difference for the case of no mixing device and the case with distribution plate is expected, as shown in Section 2.2.3. But why the swirler also gives a different result is not known, as similar flame length are expected. For higher frequencies the transfer function of the swirler and no mixing device are similar, but the phase delay of the case with distribution plate is different.

2.3 Summary

In this chapter the effect of different flames on the flame transfer function is studied. First the experimental setup and how the data is analyzed is explained and an example of the visualization is given. The Section 2.2.1 the effect of different parameters is studied, so how the flame transfer function changes with varying equivalence ratio or air speed. In Section 2.2.2 the effect of different burner pattern on the flame transfer function is studied. Sections 2.2.3 and 2.2.4 studies how distribution devices can change the flame transfer function. Chapter 3 goes into system identification of the boiler.

Chapter 3

Acoustic properties of the boiler

The goal of this study is to gain insight on how thermoacoustic oscillations occur and how to predict them. As stated in Chapter 1, typical household boilers suffer a lot form these oscillations. The problem consists of two parts, the flame, and the burner system (the boiler). In Chapter 2 the flame is studied. In this chapter the boiler itself is studied. The aim of the experiments is to investigate the effect of different parts of the boiler on the acoustic signature. This information should help to predict acoustic instabilities.

3.1 Experimental setup

In order to study the acoustic properties of the boiler, a method is developed to measure the acoustic response. In this section the that equipment is used is described, how the acoustic fingerprint is characterized and how this fingerprint is visualized.

3.1.1 Equipment

In order to measure the acoustic signature of the boiler a new method was developed. This method includes introducing an oscillation to the air in the boiler using an external acoustic source at one place and measurement of the boiler response to the range of pure tone excitations at the position of the burner. The excitation is generated by a loudspeaker connected to the inlet of the boiler. Close to where the loudspeaker is connected, a microphone is installed in the inlet. The purpose of this microphone is to monitor and control the excitation. The other microphone is installed inside the burner, which is installed in the boiler. This is possible because the burner is a cylinder, as shown in Figure 2.10a. For the microphone to be placed the inlet of the boiler needed to be adapted to hold this microphone. A overview of the setup is shown in Figure 3.1. Initially a pressure transducer was used to monitor and control the excitation. But because of the sensitivity and low-frequency noise of this transducer, it was replaced with a microphone. The microphones are identical. The specification is given in Appendix B.1.
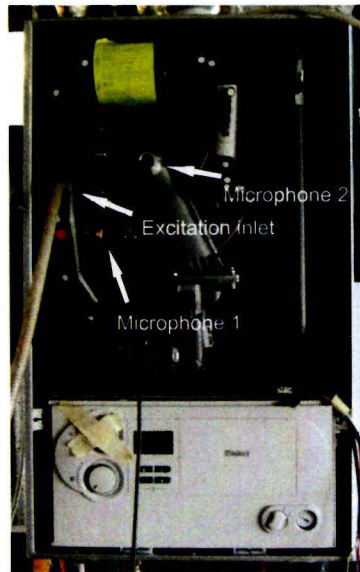
Figure 3.1: Layout of the setup for boiler measurements

The microphones and the loudspeaker are connected to a computer via a data acquisition (DAQ) card for acquiring and producing of the signals for these devices. The DAQ card (National Instruments BNC 2120) is connected to a PC with LabVIEW software which was developed to allow automated measurements and to control the excitation intensity depending upon the system response.

3.1.2   Obtaining the acoustic fingerprint

In order to measure the acoustical response of the boiler pure tone excitation is used in the boiler system. The range of frequencies used depends on if the boiler is operating or not. When the boiler is not, and thus no flame is present and the air in the boiler is stationary, the frequency goes from 30 to 1250 Hz. But when the boiler is operating the range goes from 30 to 700 Hz, as the signal to noise ratio is too low above 700 Hz. The lower limit is the result of the loudspeakers that is used.

The acoustic signature of the boiler system can be characterized by a function TF which is similar to the acoustic transfer function. Function TF relates the system response (pressure oscillations measured by microphone 2) with the excitation (pressure oscillations measured by microphone 1). As a function of f, it looks as follows:

$$TF(f) = \frac{p_2}{p_1} \tag{3.1}$$

Here $p_1(f)$ and $p_2(f)$ are signals of the first and second microphone respectively. To lower

the influence of noise on the measurements, TF (Equation 3.1) is calculated using the Fourier transformation of both pressure signals. The spectral power density was integrated in the vicinity of the excitation frequency.

3.1.3 Representation of the acoustical fingerprint

In the first part of this chapter it is explained how the acoustic fingerprint is measured and calculated. To be able to compare different acoustic fingerprints, TF as calculated in Equation 3.1 can be visualized. As TF is a complex number, the gain and the phase are plotted as a function of the frequency. For the first experiment the acoustic fingerprint is made for a boiler which is not modified and it is shown in Figure 3.2.
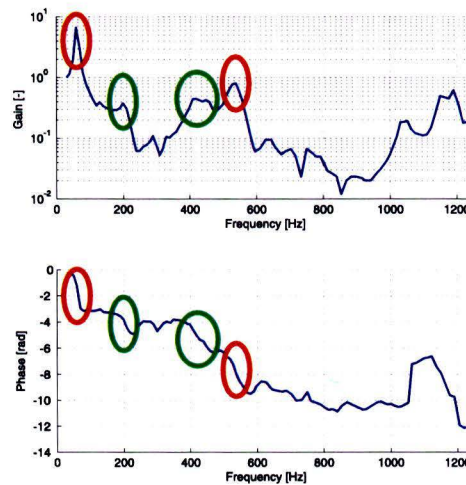
Figure 3.2: Acoustic signature of disconnected boiler

In Chapter 1 it is explained that the gain influences the growth rate of the thermoacoustic instabilities and the phase affects the sign of the growth rate. As shown in the figure, the acoustic fingerprint of the disconnected boiler is complicated as a result of the various volumes. It should be noted that the scaling of the vertical axis of the gain plot is logarithmic. This is done because the gain will be close to zero for some frequencies. In Section 3.2.4 damping is added to various parts of the boiler, which will result in lower values of the gain. It should be clear that a difference in gain is not necessarily is a result of a difference in function TF.

From a figure like Figure 3.2 the eigenfrequencies of the system can be identified, as an eigenfrequency gives a spike in the gain plot and a jump of $-\pi$ in the phase plot. However, this is the case for an ideal situation. In the results of complicated system, as shown in Figure 3.2, the peaks in the gain plot or the jumps in the phase plot are not as easy to distinguish. The eigenfrequencies which are most striking in this example are at 60 and at 540 Hz, which

are in the red circles in the figure. But also the frequencies 200, 410 and 450 Hz could be eigenfrequencies, which are in green circles in the figure. For this study an eigenfrequency is an important property of system. If the boiler is combined with the wrong burner it can result in an acoustic instability at that frequency. An eigenfrequency probably corresponds with a specific part of the boiler. This is studied in later sections.

3.2   Results and discussion

In Section 3.1 the measurement setup and processing is explained. This section presents the results of the experiments and discusses the results. The aim of the study done in this section is to investigate the influence of different parts of the boiler on its acoustic signature. During this study the boiler was installed, and the effect of this is also looked into first, as some experiments are done on the disconnected and some on the installed boiler. In the last part of this section the effects of different burners in the boiler are discussed.

3.2.1   Effect of boiler installation and ignition

For some experiments described in this chapter the boiler is not connected. For other experiments the boiler is installed. Installing the boiler means that it is connected to a gas line, integrated in a closed water circuit and a chimney is attached to remove exhaust gasses. As a result of this installation the acoustic fingerprint changes. Also igniting the boiler results in a change in fingerprint. In Figure 3.3 the comparison is made between the boiler before installation, after installation but not burning and a burning boiler.
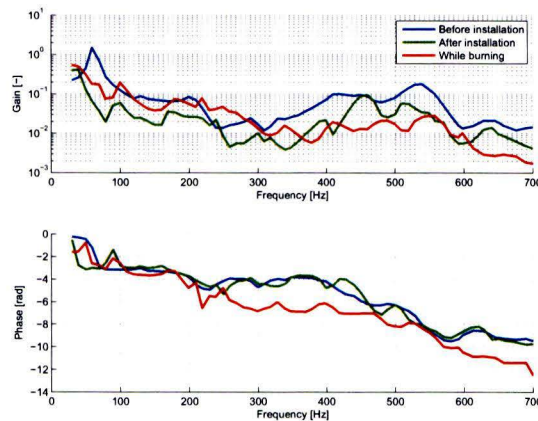
Figure 3.3: Influence of installing the boiler and ignition on the acoustic fingerprint

For frequencies lower than 200 Hz the the signature changes significantly, the spike at 60 Hz has disappeared. The fingerprint of the installed boiler has an eigenfrequency at 460 Hz, which does not seem to exist for the uninstalled boiler. This eigenfrequency is gone after ignition of the boiler. The general trend of the gain is the same for the not burning and burning boiler. Furthermore the phase delay in the case of the ignited boiler is significantly

larger in the range of 250 to 480 Hz, and also for frequencies higher than 600 Hz. With this information it is clear that the model should take into account that the introduction of a flame may change some parameters of the boiler.

3.2.2 Influence of the chimney

Section 3.2.1 studies the changes to the acoustic fingerprint as a result of installation of the boiler. The addition of a chimney is one of the significant changes made to the boiler. Also, when a boiler is installed it depends on the place on how long the chimney will be, as it connects the boiler to the environment. In this section the influence of the length of the chimney on the acoustic fingerprint is studied. For this experiment four different chimney lengths are used: no chimney, 50, 140 and 340 centimeter. This is the length of the tube attached to the boiler, as a small chimney exists between the burner vessel of the boiler and the boiler housing. The results are shown in Figure 3.4. This experiment is conducted on the disconnected boiler.
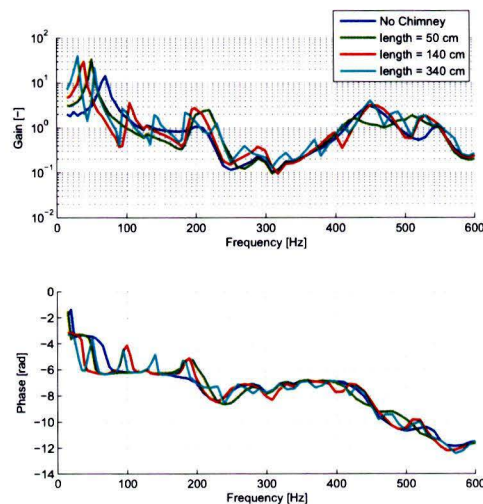
Figure 3.4: Difference in acoustic signature for different chimney lengths

From this figure it can be concluded that the chimney length has several effects on the acoustic fingerprint. The eigenfrequency, 70 Hz for no chimney, shifts to a lower frequency, 30 Hz for a chimney of 340 cm. Further it can be observed that the chimney also has an effect on the rest of the gain plot, as the chimney of 50 cm gives a different response between 400 and 550 Hz. Also it is shown that a longer chimney gives a response with more peaks. However the general trend is similar. In the range 600 to 1250 Hz the chimney length has no distinct effect on the acoustic fingerprint.

This section shows that the chimney has an effect on the stability of the boiler. As a boiler is installed in different places with a different chimney length, it can result in stable operation

in place and instable operation in the other. When a burner is tested with a boiler this effect should be taken into account.

In Section 3.2.3 the effect of different inlet lengths is studied. When the inlet length was varied each multiple of the eigenfrequency added 2π phase delay. This effect is not observed when adding length to the chimney. This is the probably the result of where the length is added. In case of the inlet, the extra length was added between the microphones, as with the chimney the length was added after the last microphone.

3.2.3 Influence of the inlet

The boiler used for the experiments in this chapter is equipped with a standard inlet tube. In this section the length of the inlet, but also the addition of holes is studied, as previous studies have proved that the hole has an influence on the acoustic fingerprint of the boiler. The original inlet that came with the boiler is about 80 cm long, with the one hole positioned near the end of the inlet at the gas valve housing. The reference microphone is positioned 20 cm before the gas valve. Different inlets have been made with a length of 40, 70 and 100 cm, with the reference microphone positioned 10, 40 and 70 cm before the gas valve housing and with one, two or three holes respectively. The first experiment studies the effect of varying length of the inlet. For this experiment all holes in the inlet are closed. This experiment is conducted on the installed boiler.
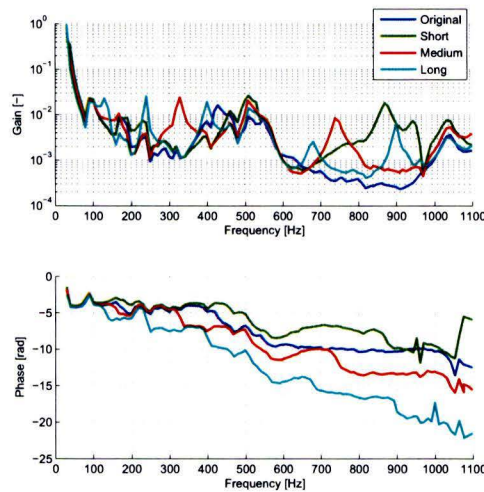
Figure 3.5: Difference in acoustic signature for different inlets

If a tube is lengthened, the eigenfrequency shifts to a lower frequency and multiples of this eigenfrequency show. This effect is also shown in Figure 3.5. Although the eigenfrequency is not clearly recognizable, lengthening the inlet results in more multiples. The length also has an effect on the phase delay. However, for almost the whole range the difference is 2π, so

it does not have a influence on the stability of the system. When designing an inlet for the boiler, it should be realized that a longer inlet creates more multiples of the eigenfrequency and more potential unstable frequencies. On the other hand, a small change in inlet length can result in making the system stable as the multiple changes.

Previous studies showed that a hole in the inlet could have an influence on the acoustic fingerprint of the boiler. In this section the influence the number of holes in the inlet is studied.
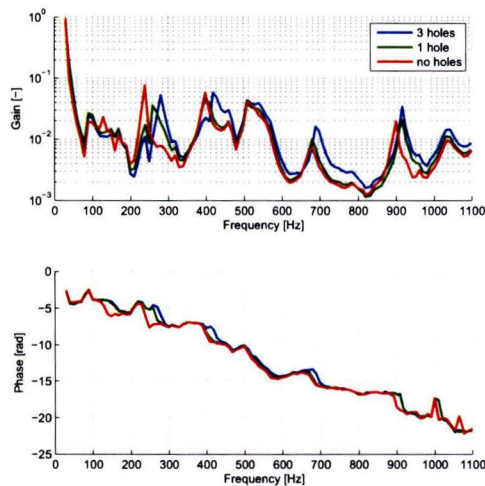
Figure 3.6: Difference in acoustic signature for different inlets

In Figure 3.6 the results are shown. Adding holes to the inlet has little effect, only the resonance frequencies shift to higher frequency. The biggest shift is around 250 Hz, where the frequency shifts from 240 for no holes to 280 Hz for three holes.

3.2.4 Recognizing the influence on the boiler acoustics of other contributing parts

It is expected that the different components have a specific effect on the acoustic fingerprint of the boiler. In order to determine which part has an effect, or which parts have the biggest effect, damping is added to that part using foam and the acoustic fingerprint of this experiment is compared with the result from the case with no damping.

The results are shown in Figure 3.7. In this figure, only components are compared which have an influence on the acoustic fingerprint. Also only the relevant part of the graph is shown; the part where the acoustic fingerprint diverges from the situation without damping. It can be concluded that three parts of the boiler have an influence on the acoustic fingerprint. Adding damping to the exhaust, which is between the burner vessel and chimney, only has an effect

Figure 3.7: Influence of damping on parts of the boiler

at frequencies lower than 200 Hz. Adding damping before the fan, at the end of the inlet, results in lower responses at frequencies higher than 800 Hz. It also results in a downward peak at 960 Hz. If damping is added to the pipe that connects the fan with the burner, it results in a different response for several frequencies. The small positive peak at 200 Hz for the undamped situation changed to a negative peak for this damped situation and the eigenfrequencies at 540 and 1040 Hz have disappeared.

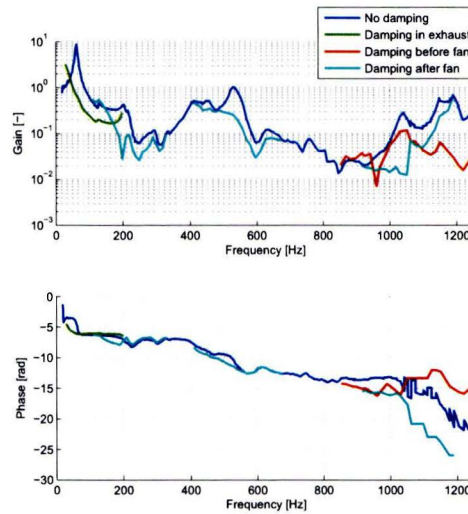This information can be used when validating the model of the boiler. This result indicate not every part of the boiler needs to modeled very accurately. Creating the model is discussed in Chapter 4.

3.2.5   Influence of different fan speeds

To get an air-fuel mixture in the burning chamber, a fan sucks in air which passes a venturi tube, where gas is inserted. Then the mixture passes the fan and it blows this mixture towards the burner. A higher fan speed results in more air and fuel in the combustion chamber and thus in a higher burning intensity. Because it was not known if the fan has an influence on the acoustic fingerprint, it is studied in this section. This experiment is conducted on the disconnected boiler. The fan speed is varied between zero and 4480 rpm. The highest fan speed corresponds to the maximum power output of the boiler, namely 20 kW. For this experiment the boiler is modified in order to manually set the fan speed.

The results are shown in Figure 3.8. From this figure can be derived that the fan speeds has no significant effect on the acoustic fingerprint. However, measuring the signature with a higher fan speed is more difficult. The fan increases the noise in the system which reduces the signal-to-noise ratio.
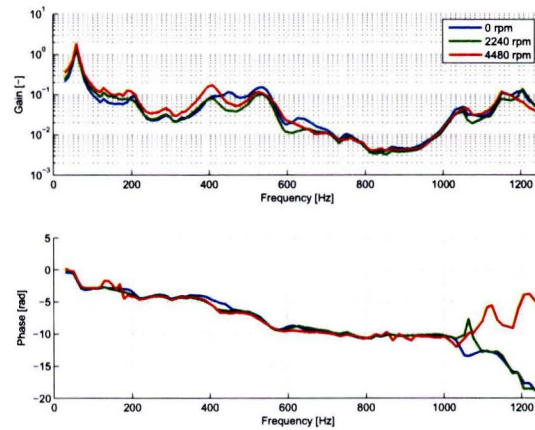
Figure 3.8: Influence of the fan on the acoustic fingerprint of the boiler

3.2.6 Effect of different water temperatures

Several parameters of the boiler can have an effect on the acoustic fingerprint, but can also change over time. One of these parameters is the temperature of the water in the boiler. By experience of burner manufacturer Polidoro, some burners cause acoustical oscillations when the boiler starts up, which means everything is at room temperature when ignition occurs. Then the oscillations last until the system is warmed up, which takes about 10 seconds. In the boiler the water is warmed in a heat exchanger. By increasing or decreasing the flow the water temperature in the heat exchanger can be controlled.
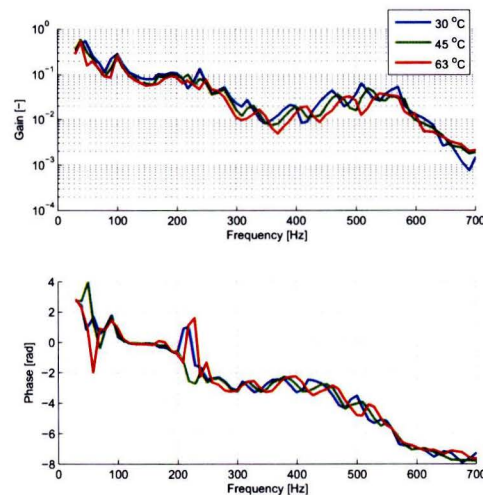
Figure 3.9: Influence of the water temperature on the acoustic fingerprint of the boiler

The results are shown in Figure 3.9. The responses for the different water temperatures are similar, but for a higher water temperature peaks shift to a higher frequency between the range of 300 to 600 Hz. The difference in frequency at which the peaks occur seems to be constant. The experiments where done with a step size of 10 Hz, so an experiment with a smaller step size should be conducted to get more information on why this phenomenon occurs.

3.2.7   Effect of flame parameters

In Chapter 2 the influence of several parameters of the flame on the flame transfer function was studied. Now that the boiler is installed and running, it is interesting to see what effect a variation in flame parameters has on the acoustic fingerprint of the boiler. The parameter varied here is the equivalence ratio. To determine the equivalence ratio of the air-fuel mixture, an exhaust gas analyzer was connected to the boiler. As the composition of natural gas is known, the equivalence ratio can be calculated.
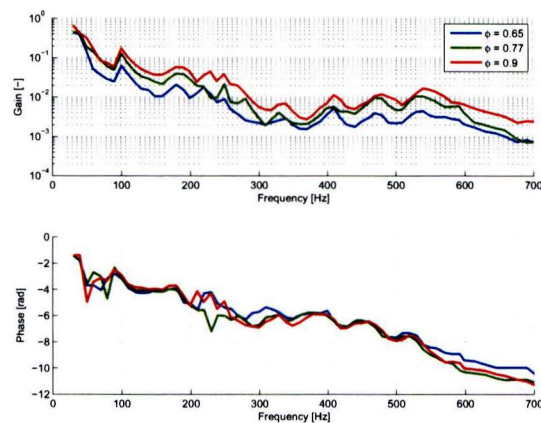
Figure 3.10: Influence of the equivalence ratio on the acoustic fingerprint of the boiler with 2240 rpm

In figure 3.10 the results are shown for the working boiler. It can be concluded that with the experimental setup used for the boiler system identification it is not possible to measure the influence of flame parameters, because there is little variation between the different measurements. For a better prediction of acoustic instabilities with the combination of the flame information and the acoustic signature, a model is necessary.

3.3   Summary

In this chapter the acoustic properties of the boiler are studied. For this goal a setup was created using a typical household boiler which was fitted with measurement equipment. The boiler was installed and the influence of running the boiler is studied. These involved physical

properties of the boiler like a varying chimney length and inlet length. The chimney changes the lowest eigenfrequency and with the inlet the frequency of the multiples can be varied. Non-physical properties are varied, like added damping to parts of the boiler to determine which part of the boiler corresponds to which part of the acoustic signature, varying water temperature which proves that there is a difference between startup and continuous operation, and the effect of the different fan speeds to check its influence when burning. In the last section of this chapter a flame parameter was varied to see if the effect of changes to the flame can be measured in this setup. This experiment shows that both types of experiments are necessary to get all the information for instability prediction. In Chapter 4 a start is made on a model of the boiler in order to make a more accurate prediction of the acoustic instabilities.

Chapter 4

System modeling

The household burner devices are very sensitive to acoustic instabilities. This study aims to get more insight in this topic. As the problem consists of 2 elements, namely the flame and the acoustics of the boiler system, these elements where studied in Chapter 2 and Chapter 3 respectively. These chapters present information by which acoustic instabilities can be predicted. However, for a more accurate prediction it is necessary to create a model of the system and the flame. This chapter explains how the modeling software works. A simple test is done to verify the performance of the model and a simple model of the boiler is created.

4.1 Acoustic system

In Chapter 1 the acoustic Riemann invariants f and g are introduced to describe the solution structure in terms of harmonic disturbances that propagate with and against the mean flow. In this section the structure of a program is presented that calculates the behavior of an acoustic system in terms of the Riemann invariants.

An acoustic system consists of various elements (e.g. ducts, diffusers, combustion chamber, ...) and nodes (connections between elements, e.g. area change, trijunction, ...). For each element and some nodes an expression can be given in terms of the Riemann invariants f and g. Several of such elements are described in [13]. The equations in terms f and g of the several elements and nodes can be combined in a system of equations and solved for the Riemann invariants, which describe the acoustical behavior of the system.
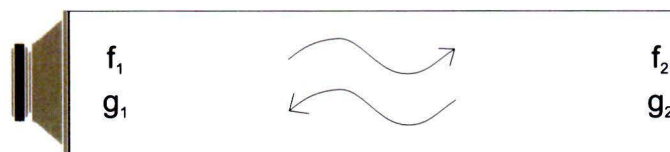

Figure 4.1: Sketch of a simple acoustic setup

It is convenient to explain this more clearly with an example. In Figure 4.1 a simple system is depicted, which consists of a tube that is open at one end and closed with a loudspeaker at the other end. This system has two connecting nodes, one node between the loudspeaker and the tube and the other node between the tube and the open end.

The loudspeaker provides a boundary condition for the velocity $u(x = 0) = U \exp(i\omega t)$, which is expressed in Riemann invariants as:

$$f_1 - g_1 = U. \tag{4.1}$$

The open end also provides a boundary condition, as $p(x = L) = 0$, or in terms of f and g,

$$f_2 + g_2 = 0. \tag{4.2}$$

The acoustic behavior of the tube connecting the loudspeaker and the open end can be described by two equations:

$$\begin{aligned} f_2 &= e^{-i\omega L/c} f_1, \\ g_2 &= e^{i\omega L/c} g_1. \end{aligned} \tag{4.3}$$

The above equations (Equation 4.1, 4.2, 4.3) can be combined in a system matrix:

$$\begin{pmatrix} 1 & -1 & 0 & 0 \\ 0 & 0 & 1 & 1 \\ -e^{-i\omega L/c} & 0 & 1 & 0 \\ 0 & -e^{i\omega L/c} & 0 & 1 \end{pmatrix} \begin{pmatrix} f_1 \\ g_1 \\ f_2 \\ g_2 \end{pmatrix} = \begin{pmatrix} U \\ 0 \\ 0 \\ 0 \end{pmatrix} \tag{4.4}$$

This equation consists of a system matrix (A) and a vector of unknowns (f_i, g_i's) on the left side and the system vector on the right side. With the system of equations in 4.4 there is an inhomogeneous (driven) system which can be solved for the values of the f_i, g_i's, but only when the determinant of system matrix A is not zero. The acoustic response can be found by solving the system for a range frequencies at a position in the system where a node is defined.

For a homogeneous system the equation $Det(A) = 0$ gives the eigenfrequencies, at which the system is in resonance. The equations used to create system matrix A are the same for the homogeneous and inhomogeneous system.

As a single acoustic element will only concern a few Riemann invariants, most elements in the system matrix will be zero; the system matrix will be a sparse matrix. The system vector describes the excitation in the system and as excitation will (most likely) happen only at one node, the system vector will only have one non-zero element.

4.2   Model

In Section 4.1 is described how an acoustic system can be modeled. This section explains
how a software model can be created which can easily be modified.

For the modeling Matlab Simulink is used. Simulink is a toolbox in which provides a graphical
environment in which customizable blocks can be used. This software was designed at the
TU/e, but during this study the software is expanded in order to calculate the frequency
response. As each acoustic element and node can be expressed in terms of f and g, a library
of blocks for the acoustical elements is made. The simple system that is shown in Figure 4.1
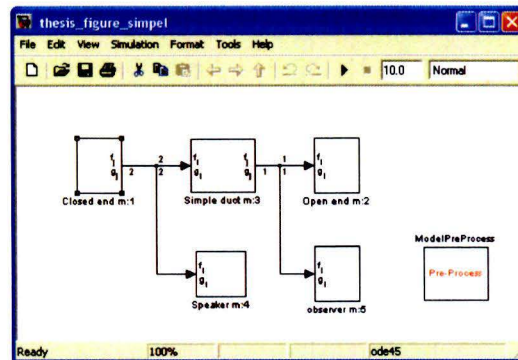is build in Simulink and shown in Figure 4.2.

Figure 4.2: Simulink model of the simple acoustic setup

To explain how the modeling software works, first only the closed end, simple duct and open
end are evaluated. Between these three elements there are two connections, so there are two
pair of f and g and the size of the system matrix is four by four. Each block holds the
equations which represent that element. In the figure in the right bottom corner the block
"ModelPreProcess" can be seen. When the model is saved, this block numbers all connections
which corresponds with the f_i, g_i's. In the figure connection '1' is between the simple duct
and the open end and thus f_1 and g_1 go with this connection. After the numbers are assigned,
the simulation is started. With this the system matrix and the system vector are created, but
also the block parameters are saved, like medium (air, methane, ...) and temperature from
which the speed op sounds is derived. Because this system, with only a closed end, simple
duct and open end, is homogeneous, solving for $Det(A) = 0$ will give the eigenfrequencies.

To create an inhomogeneous system, excitation has to be introduced in the model. This done
with the block Speaker in Figure 4.2. When is simulation is started, this block looks up to
which line it is connected. Then this block adds the excitation to the system vector. The
advantage of adding the excitation in this way is that the not only a loudspeaker can be
modeled (closed end with excitation) but also excitation can be added in the middle of a tube
like in case of the boiler in Chapter 3.

For a frequency response it is necessary to know for what node the system of equations should be solved. For this the observer block is introduced. The observer block works similarly as the speaker block, as it also looks to which to which line it connected. When it is known to which line it is connected, it is also known which f and g should be used to calculated the pressure or velocity response. With both the Speaker block and the Observer block the system can be solved. The frequency response of the system can be calculated by solving for various frequencies. Each frequency gives a different solution, and the frequency response can be calculated for a range of frequencies.

4.3   Model validation

In Section 4.2 is explained how the Simulink model works. In this section the modeling software is tested using a simple experiment. The experimental setup is explained as well as the simulation parameters.

4.3.1   Experimental setup

For this experiment a new setup is created. As this experiment is only to verify the basic functions of the modeling software as well as the modifications made (the loudspeaker and observer form Section 4.2), the setup is simple.

The basis of the experiment is a PVC tube with an inner diameter of 4,5 cm and 65 cm long. At one end of the tube, at 6,5 cm from the end, a hole is made to connect the loudspeaker as in the boiler setup shown in Figure 3.1. At 7,5 cm from the end a hole is made to insert a microphone. On the other end of the tube, also at 7,5 cm from the end, a hole made for the other microphone. The ends of the tube can be acoustically closed with plugs. The microphones and loudspeaker are measured and modulated in the same way as with the boiler setup. The microphones are connected via a DAQ card and the loudspeaker via a amplifier to a DAQ card to a computer. In order to measure the acoustical response of the boiler pure tone excitation is used.

4.3.2   Results

The Simulink model would look similar too the model shown in Figure 4.2, but with two extra simple duct blocks, inserted between the closed end on the left side and the line that leads to the speaker and on the other side between the line that connects to the observer and the open end. The dimensions of the experimental setup are copied into the software model. The open end and closed end blocks can be changed depending on if the ends on the setup are closed or not. For this experiment, the end where only one microphone is connected is either closed or open.
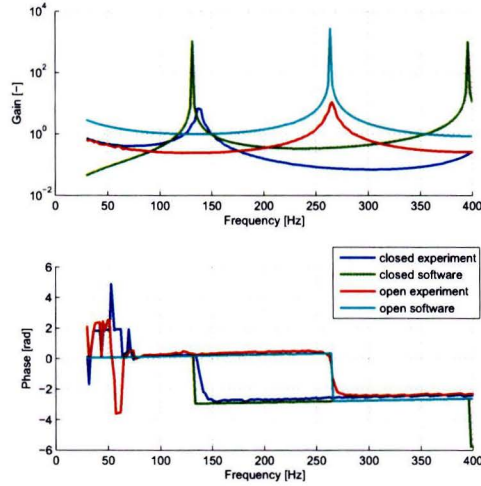
Figure 4.3: Comparison of the experiment with the software model

The results are shown in Figure 4.3. There are a few things that can be concluded from this figure. First is the prediction of the eigenfrequencies. The eigenfrequency of a tube with two open (and two closed) ends can be determined by:

$$f_{eig} = \frac{1}{2}\frac{c}{l}. \tag{4.5}$$

Here, c is the speed of sound, 343 m/s at room temperature and l is the length of the tube. In this case this results in an analytical eigenfrequency of 264 Hz. The software gives an eigenfrequency of also 264 Hz, while the experiment gives 266 Hz. For the experiment with one end closed, the analytical eigenfrequency can be obtained by:

$$f_{eig} = \frac{1}{4}\frac{c}{l}, \tag{4.6}$$

which gives 132 Hz. The model also gives 132 Hz, while experiment gives 138 Hz. At 396 Hz a spike can be seen for the case with one closed end for the model calculation. This is a multiple of the eigenfrequency, three times the eigenfrequency. If the measurement range of the experiment extended to at least 414 Hz (three times the eigenfrequency), this spike would also have been visible in the experimental results. The small differences between the model and the experiment can be caused by an measurement error with the length of the tube.

If the phase delay of the model and the experiment are compared, it can be concluded that both signals are similar. At the point of the eigenfrequencies, which are calculated above, there is a jump of $-\pi$, as expected. Biggest difference is the inaccurate calculation of the

phase delay for the experiments at low frequencies. This most likely the result of the inaccurate tone generation of the loudspeaker combined with the data processing.

With this it is clear that the modeling software works. The software is able to predict the properties of the (simple) system. The adaptations to the software make it possible to introduce excitation to the model and determine the frequency response at any point in the system.

4.4   Boiler model

In Section 4.3 the modeling software is validated. In this section a start is made with a model of the boiler. As shown in Chapter 3 the frequency response of the boiler suggests that creating a model of the boiler is difficult. This section does not present a complete model of the boiler, but a start is made.

In order to create a model, the measurements of the boiler were taken. These measurements are the basis of the model. In Figure 4.4 the Simulink model of the boiler is shown. Although it is tried to make a copy of the boiler in the model, for some features it is not known how to include them in the model. It is not know what exact effect the fan and the burner have on the frequecy response. For this further research is necessary. Further is the position of the loudspeaker similar to that of the reference microphone in Figure 3.1.
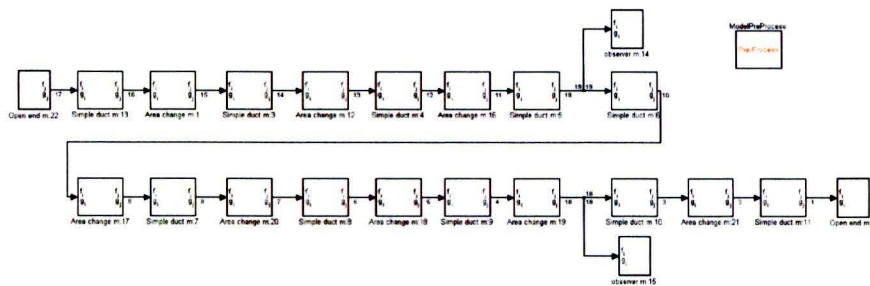

Figure 4.4: Simulink model of the boiler

In Figure 4.5 the frequency response of the model of the boiler is plotted together with the acoustic signature of the boiler as it is measured. First the gain of the frequency response is compared. When taking into account the many elements used in the model, the response of the model is not too far off. Not only the general trend is similar, but there is also a eigenfrequency at a low frequency.

Although the general trend is similar, there are still some major differences between this model and the acoustic fingerprint of the boiler. In Chapter 3 it is described that different parts of the boiler are directly linked to the acoustic fingerprint. There are several reasons
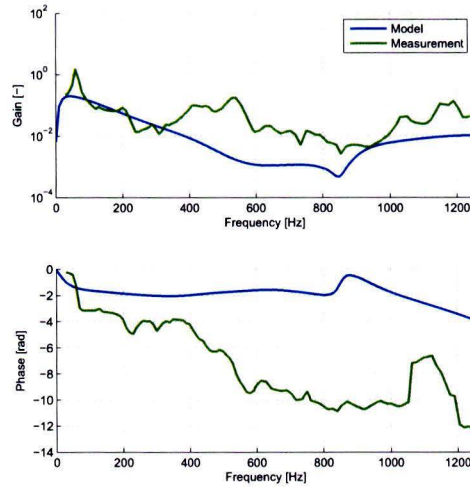
Figure 4.5: Comparison of the acoustic signature of the boiler with the software model

why the model is off compared to measurements. In Figure 4.5 the effect of the individual parts is not visible. Several elements may cause damping, such as the hole in the inlet and the heat exchanger outside the burning chamber may also cause an acoustic effect, which are both not included in the model. The different elements of the boiler are modeled as simple ducts, but it should be checked if this is valid. When the individual elements are correctly modeled, the interaction between the different elements needs to be studied.

4.5 Summary

The aim of this thesis is to gain more knowledge about acoustic instabilities from the flame and the system in order to predict these instabilities. The next step in this study is creating a model for more accurate prediction. Section 4.1 explain how from equations of elements a system is constructed which can be solved. Section 4.2 goes into how the software constructs this model and that elements are added to calculate the frequency response of a model. In Section 4.3 a simple experiment is conducted in order to validate the model but also the elements that were added. In Section 4.4 a start is made with a complete model of the boiler. Although this first model has some good point, future research should improve this model for more accurate instability prediction.

Chapter 5

Conclusions and Recommendations

5.1 Conclusions

The aim of this study is to get more insight in the thermoacoustic instabilities in a burner system, and more specific a household burner device. With this insight it should be possible to predict instabilities, which helps the company that designs burners to find the right burner for the boiler. As the thermoacoustic instabilities are the result of combination of the burner and the boiler, both are studied. In Chapter 2 the effect of different parameters on the burner are studied. In Chapter 3 the boiler is studied. In Chapter 4 a start is made with modeling of the burner system that is studied, which is used for a more accurate prediction of the instabilities.

First the effect of the flame in the burner system is studied. The flame can be varied with different parameters like equivalence ratio and velocity. This gives differences in the flame transfer function which characterizes the burner system. It is shown that different patterns, although the same porosity, have a different acoustic signature. Further devices introduced to enhance the uniformity of the flame on the burner deck are studied. These devices include a swirler plate and a distribution plate and have an effect on the flame transfer function. The porosity of the distribution plate is an important parameter, as well as the distance of the distribution plate to the burner. By varying the parameters of the flame these devices, a desired flame can be created which in combination with the burner system does not cause acoustic instabilities.

For studying the boiler a setup was created to introduce excitation and measure the frequency response. For several parts of the boiler the effect on the frequency response is measured. The exhaust has a big effect on the eigenfrequency at lower frequencies, which is an important effect as the exhaust length can vary for every installed boiler. Furthermore the inlet and several elements of the boiler have a noticeable effect on the acoustic properties of the boiler. After the boiler was installed, the effect of ignition is studied, as well as the temperature of the water in the heat exchanger. As both change the acoustic signature of the system, they should be taken into account when combining a burner with the boiler.

As information about the flame and the burner system are used for (in)stability prediction, for a more accurate prediction a model is needed. Software developed at the Eindhoven University of Technology is used and modified in order to calculate the acoustic response of the model. The software and the addition are validated with an experiment. A start is made on the boiler model.

5.2   Recommendations

For measurements of the acoustic properties of the flame pure tone excitation is used. Each sweep takes several minutes. The processing of the data is also quite time consuming and a lot of time can be saved by optimizing these processes.

Although a lot of measurements were done on the boiler using two microphones, the acoustic impedance cannot be measured. If the impedance can be measured a direct analysis can be given on the acoustic stability of the boiler.

For a more accurate prediction of the acoustic instabilities the model should be finished. The software used for the modeling should be evaluated to check if an element in the software gives the same response as the corresponding element from the boiler.

Bibliography

[1] A. Putnam, *Combustion Driven Oscillations in Industry*. New York: Elsevier, 1971.

[2] S. Candel, "Combustion dynamics and control: Progress and challanges," *Proceedings of the Combustion Institute*, vol. 29, pp. 1–28, 2002.

[3] T. Lieuwen, "Modeling premixed combustionacoustic wave interactions: A review," *Journal of Propulsion and Power*, vol. 19, No. 5, 2003.

[4] V. Kornilov et al., "Experimental and numerical investigation of the acoustic response of multi-slit bunsen burners," *Combustion and Flame*, no. 156, pp. 1957–1970, 2009.

[5] V. Kornilov et al., "Thermo-acoustic behaviour of multiple flame burner decks: Transfer function (de)composition," *Proceedings of the Combustion Institute*, no. 32, p. 13831390, 2009.

[6] Lord Rayleigh, *The Theory of Sound, Volume 2*. Courier Dover Publications, 1945.

[7] G. Markstein, *Nonsteady Flame propagation*. New York: Pergamon Press, 1964.

[8] V. Kornilov, *Experimental Assessment of the Acoustic Response of Laminar Premixed Bunsen Flames*. PhD thesis, Eindhoven University of Technology, 2006.

[9] T. Poinsot and D. Veynante, *Theoretical and Numerical Combustion*. Philadelphia: Edwards, 2001.

[10] M. Munjal, *Acoustics of Ducts and Mufflers*. New York: John Wiley & Sons, 1987.

[11] N. Noiray et al., "Self-induced instabilities of premixed flames in a multiple injection configuration," *Combustion and Flame*, vol. 145, Issue 3, pp. 435–446, 2006.

[12] N. Noiray et al., "Passive control of combustion instabilities involving premixed flames anchored on perforated plates," *Proceedings of the Combustion Institute*, no. 31, pp. 1283–1290, 2007.

[13] W. Polifke, J. van der Hock, and B. Verhaar, "Everything you always wanted to know about f and g."

Appendix A

Flame transfer function

In chapter 2 the flame transfer function is studied. In this appendix some extra information about the setup and or some extra results are given for clarification of that specific subject.

A.1 Differences in burners with distribution plate

In section 2.2.3 the influence of the distribution plate on the flame transfer function is studied. The pictures in figure A.1 show the differences in layout of the burner plates used for the first experiment in that section.
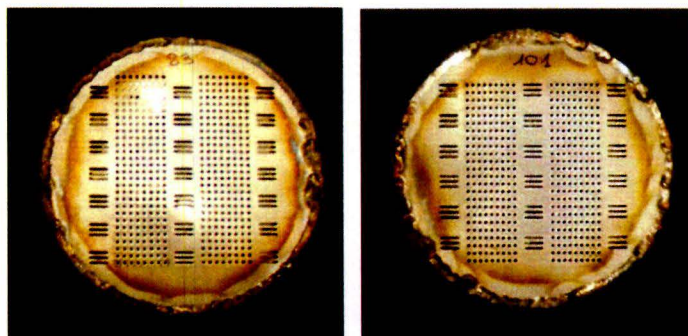
(a) Pattern 83   (b) Pattern 101

Figure A.1: Two burner patterns

A.2 Visual effect of distribution plate on burner

In Section 2.2.3 the influence of the distribution plate on the flame transfer function is studied. The distribution plate has a visual effect on the flames, which is shown in Figure A.2.

Figure A.2: Two views on the visual effect of the distribution plate on the flame

Appendix B

Acoustic properties of the boiler

In Chapter 3 the acoustic signature of the boiler is studied. In this appendix some extra information about the setup and or some extra results are given for clarification of that specific subject.

B.1 Specification of the microphones

In Section 3.1 the measurement setup of the boiler is explained. In this setup microphones are used. In Figure B.1, the specification of the microphones is shown.

Photos	
Diameter	1/2"
Standards (IEC61672)	Class II
Microphone	MP215
Optimized	Free Field
Preamplifier	MA231(TEDS optional)
Frequency Response (Hz)	20 ~ 12.5k
Open-circuit Sensitivity (mV/Pa) (±2dB)	40
Output Impedance (Ω)	< 110
Dynamic Range (dBA)	23 ~ 135
Inherent Noise (dBA)	< 23
Operating Temperature (°C)	-20 ~ 80
Operating Humidity (RH)	0 ~ 95%
Temperature Coefficient (dB/°C)	<± 0.3 dB (0 ~ 40 °C) with 250Hz, at reference temperature 23 °C
Humidity Coefficient (dB/%RH)	0.007
Pressure Coefficient (250 Hz) (dB/kPa)	-0.03
Length (mm)	91
Input Connector	BNC
Corresponding Model with TEDS	MPA265

Figure B.1: Specification of the microphones used for boiler measurements